



**HAL**  
open science

## Dynamic Study of Coupled Heavy Hydrocarbon Pyrolysis and Combustion

Nicolas Gascoin, Philippe Gillard

► **To cite this version:**

Nicolas Gascoin, Philippe Gillard. Dynamic Study of Coupled Heavy Hydrocarbon Pyrolysis and Combustion. Combustion Science and Technology, 2012, 184 (12), pp.2136-2153. 10.1080/00102202.2012.703729 . hal-00766435

**HAL Id: hal-00766435**

**<https://hal.science/hal-00766435>**

Submitted on 18 Dec 2012

**HAL** is a multi-disciplinary open access archive for the deposit and dissemination of scientific research documents, whether they are published or not. The documents may come from teaching and research institutions in France or abroad, or from public or private research centers.

L'archive ouverte pluridisciplinaire **HAL**, est destinée au dépôt et à la diffusion de documents scientifiques de niveau recherche, publiés ou non, émanant des établissements d'enseignement et de recherche français ou étrangers, des laboratoires publics ou privés.

Dynamic study of coupled heavy hydrocarbon pyrolysis and combustion.

N. Gascoin<sup>a\*</sup>, P. Gillard<sup>a</sup>

<sup>a</sup>PRISME, IUT Bourges, 63, avenue de Lattre de Tassigny – 18000 Bourges, France

## Abstract

Hypersonic flight over Mach 5 should be achieved with Supersonic Combustion Ramjet. The regenerative cooling presents the advantage to use the fuel as a coolant, which results in its pyrolysis. Both cooling channel and combustion chamber are studied numerically by coupling the transient phenomena with detailed pyrolysis and combustion chemistry (360 species and 2777 reactions). A Mach 6 flight configuration is chosen to study the impact of fuel mass flow rate on the combustion for equivalence ratio varying from 0.01 to 1. The time characteristics of the phenomena are determined. A higher flow rate provides higher hot gases temperature and faster stabilization time and auto-ignition delay. This impacts positively the flame anchoring. Several analytical laws are proposed for later development of a control strategy. A hysteresis is found because of the heat transfer dynamics. Finally, the combustion mechanism is applied and validated experimentally for kerosene pyrolysis application.

## Keywords

Regenerative cooling; Hydrocarbon pyrolysis; Supersonic Combustion Ramjet; Kerosene combustion; Detailed chemistry.

**Short Title:** Dynamic study of fuel pyrolysis and combustion

---

\* Corresponding author. Tel.: +33.248.238.473; fax: +33.248.238.871. *E-mail address:* [Nicolas.Gascoin@bourges.univ-orleans.fr](mailto:Nicolas.Gascoin@bourges.univ-orleans.fr) (N. Gascoin)

## 1. Introduction

Hypersonic flight (over Mach 5) is expected to be achieved in the coming years by means of supersonic combustion ramjet (SCRamjet) (Fry, 2004). This produces a dramatic heating, which is added to the heat flux coming from the combustion heat release. Even composite materials could not withstand such large heat load (Bouchez, 2008). Furthermore, the time allocated for the combustion in SCRamjet mode is about 1 ms (Gascoin, 2010). The thermal management of the overall vehicle and more specifically of the combustion chamber (CC) is thus an important focus for the aerospace research (Falempin, 2004). In this framework, the COMPARER program (COntrol and Measure of PArameters in a REacting stReam) has been settled by MBDA-France and by the University of Orléans (France) (Gascoin et al. 2009; Abraham, 2009). An integrated solution of regenerative cooling using the fuel is considered. Hydrocarbons are preferred for flight Mach number under 8 (Yu, 2001).

The hydrocarbon fuel is injected in a channel whose structure is preferably in ceramic matrices composite (Bouchez, 2006). A counter-flow heat exchanger is thus available towards the burned gases. When heated above 800 K, the fuel is pyrolysed and thanks to its endothermic behavior, it increases the active cooling of the hot walls (thermal energy converted into chemical one). This pyrolysis produces lighter hydrocarbon species with shorter auto-ignition delays than the initial fuel (a maximum of 0.1 ms is wanted). The chemical composition of pyrolysed mixture is complex and it requires to be specifically treated. More than hundred of compounds are produced (Gascoin, 2010). A wide spectrum of pyrolysis conditions is covered in studies of the open literature (fluid nature, conditions of temperature/pressure/residence time, open/close reactors, dilution ratio, experimental/numerical work,...) (Pant and Kunzru, 1996; Wang et al., 2008; Herbinet et al., 2007; Nageswara and Kunzru, 2006; Yu and Eser, 2000; Wang et al., 2009). Abraham (2009) proposes a deep review of this chemical phenomenon.

The pyrolysis and combustion phenomena are studied in the present paper to observe the impact of fuel mass flow rate on their coupling in order to prepare the latter step of SCRamjet engine control. Controlling the system is still a challenging task and no specific work is available in open literature to the authors' knowledge. The complete system is a coupled process in which the engine thrust depends on the chemical fuel composition injected in the combustion chamber. This composition is linked to thermal heat flux, which is applied on the cooling channel depending on the combustion itself. Because of this interaction, it is of primary importance to have information during the flight about the fuel composition (Gascoin et al., 2009; Abraham et al., 2009). On the basis of this chemical composition and of the fuel mass flow rate, it is then possible to predict the combustion (Gascoin, 2010) and hopefully to manage the thrust. The regulation of such process is not obvious for the following reason. The thrust is related to the mass flow rate and its increase may not conduct to a thrust increase because it could be accompanied by a lower pyrolysis due to lower available quantity of thermal energy per kilogram of fuel. If the corresponding chemical species present slower auto-ignition delay, an extinction of the engine is possible. This is due to the binary role of fuel in such cooling/burning system. This point is the core of the present study.

The RESPIRE code (a French acronym for SCRamjet Cooling with Endothermic Fuel, Transient Reactor Programming) has been developed and extensively validated since 2004 for this purpose (Gascoin et al., 2007; Gascoin et al., 2008; Gascoin et al., 2009). This one dimensional software is able to simulate the hypersonic vehicle cooling. It generally considers detailed n-dodecane pyrolysis mechanism (1185 reactions, 153 species) (Dahm et al., 2004) but other fluids can be studied with appropriate mechanism. The n-dodecane is used because of its purity and because it is representative of aeronautic kerosene. It is also used for the experiments which serve as validation data notably (Gascoin, 2010; Abraham, 2009). The detailed combustion

kinetic mechanism of Dagaut and Cathonnet (2006) (1592 reactions, 217 species) has been chosen among several mechanisms (Zeppieri et al., 2000; Vasu et al., 2009; You et al., 2009; Imbert et al., 2008; Kumar and Sung, 2007) for accuracy and reliability reasons. To the author's knowledge, RESPIRE (running on a Personal Computer) is one of the rare engineering and research tool able to consider the detailed chemistry, which drives the overall system. Using complete chemical scheme, particularly for complex and heavy hydrocarbon fuels like kerosene, is necessary because the combustion (diffusion flame) is fast and transient.

The aim of this paper is to observe the effect of mass flow rate variations to give first assessments on the requirements which should be met by future thrust regulation strategy. After a brief presentation of the RESPIRE code in section 2, the section 3 is dedicated to the numerical results obtained for several fixed (section 3.1.) and varying (section 3.2.) values of mass flow rate. Apart this work, the section 3.3. is related to the test of the Dagaut and Cathonnet combustion mechanism to consider the pyrolysis of decane and of kerosene with comparison to experiments. This aims at limiting the computation cost by considering a single mechanism instead of two and at improving the code efficiency.

## **2. Equations of the numerical code**

Extended details concerning the REPIRE code, the assumptions and the grid dependency can be found in 0. Its validation has been conducted under transient and stationary conditions with analytical, numerical and experimental cases (Gascoin, 2010; Gascoin et al., 2008; Gascoin et al., 2007). Some explanations of the geometry can be found in the work of Gascoin et al. (2007) to help understanding the simulated configuration. The coolant flows in 1-D from left to right in the cooling channel before being injected in the combustor where the burned gases flow from right to left. Both are separated by a thermally computed solid structure.

## **2.1. Simulation of the cooling channel**

This part of the code has been extensively described in previous works (Gascoin, 2010; Gascoin et al., 2008; Gascoin et al., 2007). The Navier-Stokes and energy equations are solved transiently in one dimension to determine the fluid velocity and enthalpy. The transport equation is solved for each chemical compound. Detailed dodecane pyrolysis mechanism is used in this work (1185 reactions and 153 species (Dahm et al., 2004). A more recent version (1449 reactions and 271 species) (Herbinet et al., 2007) could have been used but since the formation of Poly Aromatic Hydrocarbons is not the primary interest of the present work, the oldest smaller version has been preferred. The multi-species and multiphase physical properties (density, heat capacity, thermal conductivity and viscosity) are computed as a function of time, of temperature and of pressure. The boundary conditions for the fluid phase are the temperature, the mass flow rate and the pressure of the inlet fuel. The wall temperatures are computed by transient energy equation in solids taking the radiative, conductive and convective heat transfers. On one side of the cooling channel, the hot face temperature of the structure in contact with burned gases is used as boundary condition and the external environment is considered on the other side.

## **2.2. Combustion chamber and coupling with cooling channel**

The simulation of the cooling channel is coupled to the combustion chamber through the boundary conditions imposed, first by the chamber to the channel at the solid interface (hot face temperature) and second by the fuel composition, mass flow rate, temperature and pressure at the injection in the chamber. The air inlet is supposed to be ideally adapted. The spatially discretized Navier-Stokes and energy equations are solved as a function of time in the chamber to compute the velocity (Eq. 1) and temperature of the gases. Due to the one dimension assumption of the code, it is not possible to consider turbulence model like  $k-\varepsilon$  or others (Borghini and Destriau,

1995). For this reason analytical laws are used when necessary. For example, the heat transfer between burned gases and chamber walls are driven by the Nusselt number computed for fully developed established turbulent flow (Eq. 2) (Depecker and Inard, 1996). In addition, specific varying parameter along the chamber is used to model the fuel injection spray (which is not uniform in the inlet cross-section). More details concerning the modeling of turbulent dynamic boundary layer effect in the energy equation of the combustion chamber, assuming infinitely thin thermal boundary layer, can be found in the work of Gascoin (2010).

The net production rates of species are determined in the same way as for the cooling channel and a detailed combustion mechanism is used (1592 reactions, 217 species) (Dagaut and Cathonnet, 2006). The transport equation is solved for each chemical species. The physical properties of burned gases are tabulated. The radiative heat transfer between gases and walls is linearised and an average hot gas temperature is considered for that. This simplification avoids computing the view factors. The perfect gases law with varying physical properties is considered to compute the pressure. The transient thrust is computed by Eq. 3 and it is based on several intermediate parameters such as the dynalpie at the combustion chamber outlet (Eq. 4). The law of corresponding cross sections (Eq. 5) is used to obtain the Mach number at the engine outlet (subscript 5). An isentropic expansion of burned gases between the outlet of the CC and the one of the tail is considered with constant total pressure and temperature between both locations. It can be noticed that Eq. 5 is suitable for compressible isentropic gas flow under steady-state regime. This is a simplification in the equations set to be solved by RESPIRE. This assumption is balanced by considering the friction through a dynalpie yield  $\eta_{dyn} = D_4/D_5$ . This corresponds to a multiplication of the parameters at the nozzle exit by a factor less than one (Gascoin, 2010).

$$\frac{\partial(\rho_g \cdot V_g)}{\partial t} + \frac{\partial(\rho_g \cdot V_g^2)}{\partial x} = -\frac{\partial P_g}{\partial x} + \frac{\partial \tau}{\partial x} \quad (1)$$

$$Nu = 0,027 \cdot Re^{0.8} \cdot Pr^{\frac{1}{3}} \cdot \left( \frac{\mu_g}{\mu_{hf}} \right)^{0.14} \quad (2)$$

$$\frac{\partial F}{\partial x} = P \cdot dA = \frac{\partial \dot{m}_f}{\partial t} + \frac{\partial (\dot{m}_f \cdot V)}{\partial x} + A \cdot \frac{\partial P}{\partial x} \quad (3)$$

$$D_4 = P_4 + \rho_4 \cdot V_4^2 = P_4 \cdot (1 + \gamma_4 \cdot M_4^2) \quad (4)$$

$$M_5^2 - M_5^{\frac{2(\gamma-1)}{\gamma+1}} \cdot \left( \frac{A_{nozzleexit}}{A_{CC} \times M_4} \right)^{\frac{2(\gamma-1)}{\gamma+1}} \times \left( 1 + \frac{\gamma-1}{2} \cdot M_4^2 \right) \times \frac{2}{\gamma-1} + \frac{2}{\gamma-1} = 0 \quad (5)$$

Where 4 and 5 are the Numbers referring to combustor outlet and nozzle exit respectively, CC denotes the Combustion Chamber, f the fluid, g the burned gases in the combustion chamber, hf the hot face. A is the Cross-section area (m<sup>2</sup>), D the Dynalpie (Pa), F the Thrust (N), M the Mach number,  $\dot{m}$  the Mass flow rate (kg.s<sup>-1</sup>), Nu the Nusselt number, P the Static pressure (Pa), Pr the Prandtl number, Re the Reynolds number, t the Time (s), V the Velocity (m.s<sup>-1</sup>), x the Longitudinal axis (m),  $\gamma$  the Ratio of heat capacities,  $\eta_{dyn}$  the Dynalpie yield,  $\mu$  the Dynamic viscosity (Pa.s),  $\rho$  the Density (kg.m<sup>-3</sup>) and  $\tau$  the Friction tensor (Pa.m<sup>-1</sup>).

### 3. Combustion of pyrolysed fuel for flow rate effect investigation

A Mach 6 flight configuration is chosen (length of the combustor 1.1 m, width of 0.212 m, wall thickness of 3 mm, C/SiC structure) with n-dodecane full flow rate from 1 g.s<sup>-1</sup> to 100 g.s<sup>-1</sup> at 3.5 MPa in the cooling channel. The variables in the combustion chamber are initialized with hot conditions and the n-dodecane is pyrolysed in the cooling channel due to the CC heat flux before being injected for combustion purpose. The computations are performed for constant (section 3.1.) and varying (section 3.2.) mass flow rates with different mass values to observe the ignition and the extinction of the combustion. The dynamic of heat and mass transfers and of chemistry are studied to understand the time delay between the fuel flow rate variation and the

stabilization of these phenomena. A last section (3.3.) is proposed to test the feasibility of using a combustion mechanism for the fuel pyrolysis. This is of interest to simplify the computations and to ensure the correspondence between the cooling channel and the CC. The computations are conducted over simulation time of 1 s because the distance covered by the engine in 1 s is about 2000 m (due to the Mach 6 flight configuration). A control of the engine must be achieved over much smaller timescale. The order of 1 s is reasonable.

### **3.1. Static cases of pyrolysis-combustion coupling**

A brief parametric study has been conducted to qualitatively observe the respective influence of several physical parameters on the coupling (inlet air mass flow rate, air temperature, radiative heat transfer). The air mass flow rate modifies the velocity, thus the residence time in the CC. Its main effect is found on the equivalence ratio and this will be presented later by investigating the effect of fuel mass flow rate. The radiative heat transfers play a major role in the CC because they contribute to homogenize the hot face temperature of the hot wall. Near the cooling channel inlet, the hot face temperature reaches 340 K without radiation and 495 K with radiation. Finally, the inlet air temperature has been varied from 600 K to 1000 K (Figure 1a). On the one hand, its effect is found on the time needed to reach quasi steady state in the CC (from 10 ms for inlet temperature of 1000 K to 20 ms for the one of 600 K). On the other hand, it impacts the auto-ignition delay (from 20  $\mu$ s at 1000 K to 40  $\mu$ s at 600 K). These values are not so different because of the presence of radicals in the pyrolysed mixture which are still considered in the combustion mechanism. They highly contribute to the auto-ignition of the mixture. In addition, the fuel pyrolysis inside the CC inlet which is met at 1000 K but not at 800 K or less, is responsible for the discrepancies. This shows that the chemical effect is at least as important as the temperature effect. Despite the low residence time in the CC inlet, the similar composition of 600 K and

800 K cases changes for the 1000 K case (Figure 1b). After a simulation time of 100 ms, no difference between the three cases is observed on the cooling channel (outlet fluid temperature of 1025 K for the three cases with negligible discrepancies of few degrees).

*Figure 1 should be placed here*

A full test case with a fuel mass flow rate of  $10 \text{ g}\cdot\text{s}^{-1}$  is simulated during 2.7 s (Figure 2) after initialization with closest appropriate values. The temperature distributions in the structure and in the fluids (Figure 2a) present the strong cooling effect near the cooling channel inlet. The sudden temperature increase at the CC inlet (up to 3120 K), due to the combustion, highly impacts the hot wall. The hot (CC side) and cold (coolant side) faces of this wall reach respectively 1860 K and 1650 K. The fuel starts to pyrolyse 0.5 m after the injection (which corresponds to a time of 7.2 s in the channel) for a temperature around 870 K. The total residence time in the cooling channel is about 7.6 s and the maximum fuel temperature is 1450 K. As a result, the strong production of ethylene and of ethane (Figure 2b) is even replaced by the one of methane which gets the major species at the cooling channel outlet (around 31 wt.%). Hydrogen and acetylene are formed significantly (1.7 wt.% and 1.2 wt.%). This allows reducing seriously the auto-ignition delay in the CC, about  $20 \mu\text{s}$  (Figure 2c). This time is in quantitative agreement with previous results of auto-ignition delays (Gascoin, 2010). The presence of CO (ten times less than  $\text{CO}_2$ ) at the CC outlet shows that the combustion is not complete despite it tends to be.

The temperature in the CC reaches a steady state after less than 30 ms. The heat transfer through the hot wall, from the hot face to the cold face, presents a characteristic time around 0.5 s to 1 s (time to observe a heat flux pulse from one side to the other side). The chemistry is found close to stationary state after 0.3 s (Figure 2d). This latest point is difficult to determine precisely since the overall system is not strictly at steady state (due to heat conduction). Thus, by plotting

the methane production as a function of fluid temperature (which varies during the simulation), it is seen that the CH<sub>4</sub> mass fraction does not vary too much between 0.3 s and 0.6 s (Figure 2d). Due to the low fuel velocity in the cooling channel and to heat conduction in hot wall, the fuel temperature profile is not stabilized after 2.7 s and this causes the overall system to fluctuate. These observations are of great importance because the characteristic time constants of phenomena must be taken into account into the future SCRamjet regulation strategy.

*Figure 2 should be placed here*

Similar test cases have been simulated by changing the fuel mass flow rate from 1 g.s<sup>-1</sup> to 100 g.s<sup>-1</sup>. A clear impact on the flame anchoring in the CC is found (Figure 3a, c) because no combustion for the lowest fuel flow rate is observed after 50 ms despite the initialization with high temperature (Figure 3a). The flame front reaches the CC inlet after 30 ms for the highest flow (Figure 3c). Corresponding OH profiles clearly show the flame extinction for low mass flow rate (Figure 3b) to the opposite of higher ones (Figure 3d). The corresponding simulation time are noted close to the spatial profiles (unit in second).

*Figure 3 should be placed here*

The injected fuel quantity plays a role on the ignition time (Figure 4a) which increases by lowering the mass flow; from 7.5 ms to 85 ms for 100 g.s<sup>-1</sup> and 3.5 g.s<sup>-1</sup> respectively. This is due to the lower heat release because the flame temperature decreases from 3570 K to 2770 K for these mass flow values. The ignition appears very close to the CC inlet. For the 10 g.s<sup>-1</sup> and 3.5 g.s<sup>-1</sup> cases, the ignition is located at the same position, which shows that the auto-ignition delay is driven by the fuel composition. For the 100 g.s<sup>-1</sup> case, the ignition is found even before, which also shows the temperature effect on the flame anchoring. The maximum hot face temperature increases rapidly for the higher mass flow rate because of the higher combustion heat release. No cooling effect is observed on this temperature in the range 1 g.s<sup>-1</sup> - 100 g.s<sup>-1</sup> due to the

dynamics of conductive heat transfers, which are much slower than the simulated time. However, the fuel temperature computed at the cooling channel outlet is linked to the mass flow (Figure 4b). It is lower for higher fluid flow. The maximum fuel temperature at the cooling channel outlet can be related to the mass flow through a logarithm law. This is necessary to establish a model of the cooled SCRamjet with the aim of controlling the engine. To the authors' knowledge, no work is currently available on the control of non linear PDEs with non constant coefficients (Alvarez-Ramirez et al., 2001; Christofides, 1998). Proposing analytical relationship between the physical and chemical parameters is the first step before proposing a model in the coming years.

*Figure 4 should be placed here*

The residence time in the cooling channel does not only depend on the mass flow rate because thermal and chemical phenomena play a non negligible role. An analytical relationship can be proposed between the mass flow rate and the residence time (Figure 5a). A similar law is found by linking this time to the maximum fuel temperature. No cooling effect of the fuel flow rate is found on the hot face but contrarily, the hot face temperature increases with the mass flow due to the combustion heat release (Figure 5b). This result is important because it shows that increasing the mass flow rate to increase the cooling performance of the structure is not so obvious. This is due to the dynamic of the phenomena and particularly of the conductive heat transfers.

*Figure 5 should be placed here*

### **3.2. Transient gradient of injected fuel flow rate**

On the basis of preceding stabilized operating conditions ( $10 \text{ g.s}^{-1}$ ), the mass flow rate of fuel is decreased (divided by a factor 10 with a rate of  $9 \text{ kg.s}^{-2}$  after a time of 0.3 s) and then increased (by a factor 10 at a rate of  $0.9 \text{ kg.s}^{-2}$  at a time of 1 s) to observe the transient evolution of the system. The changes of mass flow are marked on Figure 6a. The dynamic variations of the

physical and chemical phenomena are summarized in Table 1 to provide an overview. The fuel temperature in the cooling channel and the one of burned gases in the CC are stabilized after 0.3 s of simulation time (Figure 6a). The fuel temperature is surprisingly not really impacted by the decrease of mass flow and the one of gases rapidly decreases and gets stabilized after 0.26 s (decreasing gradient of  $7038 \text{ K}\cdot\text{s}^{-1}$ ). On the opposite, the effect of mass flow increase at the time equal to 1 s is rapidly observable on the fuel temperature which rises due to the higher convection heat transfer (gradient of  $786 \text{ K}\cdot\text{s}^{-1}$ ). The rate of fuel flow change ( $9 \text{ kg}\cdot\text{s}^{-2}$  and  $0.9 \text{ kg}\cdot\text{s}^{-2}$ ) has an importance, in addition to the increase or decrease trend. The effect in the CC is much higher (gradient of  $59000 \text{ K}\cdot\text{s}^{-1}$ ). The stabilization in both systems is observed for a time of 1.2 s roughly (despite a slight visible evolution from 1.2 s to 1.52 s due to the establishment of heat transfer in the hot wall). The fuel temperature is 100 K higher at the end of the simulation which shows that the steady-state is not the same before and after the mass flow variations (kind of hysteresis).

*Figure 6 should be placed here*

*Table 1 should be placed here*

This hysteresis is due to the conductive heat transfer in the hot wall whose dynamics is much slower than the one of the fluid flow or of the chemistry. Before the first change of mass flow, the temperatures of the hot wall and the cold wall are not stabilized (heating gradient of  $643 \text{ K}\cdot\text{s}^{-1}$  and of  $55 \text{ K}\cdot\text{s}^{-1}$  respectively). The strong temperature decrease in the CC at  $t=0.3 \text{ s}$  prevents temporarily the hot wall to increase. Nevertheless, the combustion continues to apply a heat flux on the hot wall, whose temperature rises again at a rate of  $237 \text{ K}\cdot\text{s}^{-1}$  and then of  $344 \text{ K}\cdot\text{s}^{-1}$  after the mass flow increase (at time of 1 s). The cold wall increases regularly at a rate rising during the simulation. The dynamic of conductive heat transfer is moderately impacted by the fluid flow.

The combustion process is directly impacted by these flow changes but the engine does not stop despite the flame anchoring is shifted toward the CC downstream (Figure 6b). The gas

temperature profiles at 0.2 s and 1.52 s are very similar which shows that the conductive heat transfers in the hot wall do not impact the CC within the simulation time. A longer simulation time should be considered to observe a possible effect but, for now, a short time is sufficient since the control of the engine should be performed on a characteristic time of the order of the second or even less due to the flight speed. The combustion at the CC inlet is confirmed to be shifted since the OH radical almost disappears after 0.3 s at the location where the flame was initially anchored. The remaining H<sub>2</sub>O content is due to primary oxidative reactions and to the inlet air. The low influence of conductive heat transfer on the CC are confirmed by looking at the OH formation gradient (Table 1), which remains stable around 260 s<sup>-1</sup> before 0.3 s and after 1.5 s. For these times, an increase of 23 % is found on the fuel conversion gradient (from 1.27 s<sup>-1</sup> to 1.56 s<sup>-1</sup>). Moreover, the hydrogen production rate rises by a factor 2 (Table 1).

The effect of conductive heat transfer is shown on the fuel decomposition (Figure 7a). The differences between the 0.2 s and 1.52 s profiles are due to the higher cold face temperature. The strong mass flow decrease conducts to a faster pyrolysis, which takes place earlier in the cooling channel (around 0.55 m instead of 0.8 m for the high mass flow rate). The hysteresis is clearly visible on the hydrogen production which increases by 60 wt.% between 0.2 s and 1.52 s. The reason is the higher cold face temperature (320 K more on the maximum temperature during the simulation). It is also interesting to observe where the maximum of species production is located, for example on acetylene formation (Figure 7b). It varies from 0.7 m to 1 m roughly and its magnitude changes in the range 0.0075 wt.% - 0.02 wt.%.

*Figure 7 should be placed here*

### **3.3. Unification of the pyrolysis and combustions schemes**

To decrease the computation time and to improve the chemical results of fuel pyrolysis (Gascoin et al., 2010), the kerosene -modeled by decane- combustion mechanism of Dagaut and

Cathonnet (2006) used in preceding sections has been tested to conduct fuel pyrolysis to be able simulating both cooling channel and CC with a single mechanism. RESPIRE is used under tubular reactor configuration to simulate experimental case (thermal steps from 823 K to 1023 K, 60 bars,  $0.1 \text{ g}\cdot\text{s}^{-1}$ , Titanium reactor with inner diameter of 4.35 mm). The numerical results are compared to experimental ones and to previous numerical ones (Gascoin et al., 2010) obtained with the dodecane mechanism proposed by Dahm et al. (2004). Two test cases, one for decane and one for kerosene, are studied. The fuel mass flow rate, the inlet pressure and temperature of the fluid and the longitudinal temperature profile applied as external heating source on the reactor, all of them measured experimentally, are used numerically as boundary conditions.

The agreement with previous experimental data (Gascoin et al., 2010) is better with the Dagaut and Cathonnet mechanism, specifically made for kerosene, than with the Dahm et al. mechanism dedicated to n-dodecane (Figure 8). The secondary reactions scheme of Dahm et al. mechanism overestimates the production of  $\text{C}_2\text{H}_4$  and under estimates other species except for  $\text{C}_2\text{H}_6$  which is fairly predicted. For all gas species ( $\text{CH}_4$ ,  $\text{C}_2\text{H}_4$ ,  $\text{C}_2\text{H}_6$ ,  $\text{C}_3\text{H}_6$ ,  $\text{C}_3\text{H}_8$ ), the disagreement between experimental and numerical results with Dagaut and Cathonnet mechanism is in the range of validity of the FTIR method used to experimentally quantify these gas products (Abraham et al., 2011). Similar results are obtained for kerosene test case.

*Figure 8 should be placed here*

The pyrolysis rate is well quantified by the Dagaut and Cathonnet mechanism (Figure 9a) for both decane and kerosene fuels. This shows its good adequacy for future coupled pyrolysis-combustion studies in SCRamjet applications. The relationship found between pyrolysis and gasification rates (Figure 9b) is again of better agreement with experiments for the Dagaut and Cathonnet mechanism than for the Dahm et al. one, especially for decane. The "linear" relationship found for decane with the Dahm et al.'s mechanism is not appropriate since this has

never been observed experimentally for decane (but only for heptane) (Gascoin et al., 2010). The numerical results for kerosene obtained with Dahm et al. mechanism overestimate too much the conversion rate. Those with the Dagaut and Cathonnet mechanism underestimate it slightly.

*Figure 9 should be placed here*

#### **4. Conclusions**

The regenerative cooling of hypersonic structures by the onboard liquid hydrocarbon fuel could suitably address the problem of thermal management and supersonic combustion in airbreathing vehicles for flight speed above Mach 5. Such technology requires to monitor and to control the fuel pyrolysis in the cooling channel. The composition of pyrolysis products impacts directly the auto-ignition delay which controls the combustion in supersonic chamber. The coupling is controlled by the coolant mass flow rate and the extinction mechanism in the CC has been shown for low mass flow rate. A higher mass flow rate favors the thrust through an increased flame temperature (equivalence ratio effect) which is directly visible on the hot face temperature. A hysteresis effect due to time constant of heat transfer in hot wall has been shown. The different time characteristics have been estimated (combustion stabilization, auto-ignition delay, heat transfer, fuel pyrolysis). Several analytical laws have been proposed to enable establishing a control strategy based on a model of the system. Thanks to the knowledge developed in this work, further relationships will now be developed and tested. An engine control program should be elaborated by adjusting fuel mass flow rate to conform to a maximum authorized hot face temperature and to a required thrust.

#### **Acknowledgments**

The present work was realized with the contribution of the city of Bourges, of the "Conseil Général du Cher", of the "Conseil Régional du Centre", of the FRED, of the FEDER, of the FSE,

of MBDA-France and of Y. Parmantier. The authors want to quote the COMPAREER team and especially Guillaume Fau and Gregory Abraham from PRISME laboratory and Marc Bouchez and Bruno Le Naour from MBDA France.

## References

G. Abraham, N. Gascoïn, S. Bernard, P. Gillard, M. Bouchez, J. Bertrand, B. Le Naour, in: 16th AIAA International Space Planes and Hypersonic Systems and Technologies Conference, Bremen, Germany, 19-22 October 2009, AIAA paper, 7373

G. Abraham, Etude et développement d'une méthode d'analyse par spectroscopie infrarouge appliquée à la pyrolyse d'hydrocarbures en conditions supercritiques et transitoires, Ph.D. Thesis, 04/12/2009, University of Orléans, France

G. Abraham, N. Gascoïn, P. Gillard, M. Bouchez, J. Anal. Appl. Pyrol., 10.1016/j.jaap.2011.03.014.

J. Alvarez-Ramirez, H. Puebla, J.A. Ochoa-Tapia, Syst. Control Lett. (44) (2001) 395-403.

Borghi R., Destriau M., (1995) "La combustion et les flammes", Editions Technip.

M. Bouchez and S. Beyer, 2006, in: 13th Hypersonics Systems and Technologies Conference, AIAA paper, 3434

M. Bouchez, F. Cheuret, P. Grenard, J.J.A. Redford, N.D. Sandham, G.T. Roberts, A. Passaro, D. Baccarella, M. Dalenbring, J. Smith, in: 44th AIAA/ASME/SAE/ASEE JPC and Exhibit, Hartford, CT, July 20th-23rd, 2008 AIAA paper, 4670.

P.D. Christofides, Chem. Eng. Sci., (53) (1998) 2949-2965.

P. Dagaut and M. Cathonnet, Prog. Energ. Combust. (32) (2006) 48-92.

K.D. Dahm, P.S. Virk, R. Bounaceur, F. Battin-Leclerc, P.M. Marquaire, R. Fournet, E. Daniau, M. Bouchez, J. Anal. Appl. Pyrol. (71) (2004) 865-881

P. Depecker and C. Inard, Lois fondamentales en génie climatique, Techniques de l'ingénieur (1996) B9055

F. Falempin and L. Serre, in: 40th AIAA Joint Propulsion Conference And Exhibit, Fort Lauderdale, Florida, 11 - 14 July 2004, AIAA paper, 3344.

R.S. Fry, J. Prop. Power (20) (2004) 27-58

N. Gascoïn, P. Gillard, E. Dufour, Y. Touré, J. Thermophys. Heat Tr., (21) (2007) 86-94

- N. Gascoin, P. Gillard, S. Bernard, E. Daniau, M. Bouchez, *Int. J. Chem. React. Eng.* (6) (2008), A7
- N. Gascoin, P. Gillard, M. Bouchez, in: 16th AIAA Hypersonic Conference, Bremen, Germany, 19-22 October 2009, AIAA paper, 7375
- N. Gascoin, Editions Universitaires Européennes (2010), ISBN13: 978-6131501074.
- N. Gascoin, G. Abraham, P. Gillard, *J. Anal. Appl. Pyrol.*, (89) (2010) 294-306
- O. Herbinet, Marquaire, P.M., Battin-Leclerc, F., Fournet, R., Thermal decomposition of n-dodecane: Experiments and kinetic modeling, *Journal of Analytical and Applied Pyrolysis*, Volume 78, Issue 2, March 2007, Pages 419-429.
- B. Imbert, F. Lafosse, L. Catoire, C.E. Paillard, B. Khasainov, *Combust. Flame* (155) (2008) 380–408
- K. Kumar and C.-J. Sung, *Combust. Flame* 151 (2007) 209–224
- K. Kumar, G. Mittal, C.-J. Sung, *Combust. Flame* 156 (2009) 1278–1288
- R.P. Nageswara, D. Kunzru, *J. Anal. Appl. Pyrol.* 76 (2006) 154-160
- KK. Pant and D. Kunzru, *J. Anal. Appl. Pyrol.* 36 (1996) 103-120
- S.S. Vasu, D.F. Davidson, Z. Hong, V. Vasudevan, R.K. Hanson, *Proc. Combust. Inst.* (32) (2009) 173–180
- Z. Wang, Y. Guo, R. Lin, *Energ. Convers. Manage.* 49 (2008) 2095-2099
- Z. Wang, Y. Guo, R. Lin, *J. Anal. Appl. Pyrol.* (85) (2009) 534-538
- X. You, F.N. Egolfopoulos, H. Wang, *Proc. Combust. Inst.* (32) (2009) 403–410
- J. Yu, S. Eser, *Fuel* 79 (2000) 759-768
- G. Yu, J.G. Li, X.Y. Chang, L.H. Chen, C.J. Sung, Investigation of Kerosene Combustion Characteristics with Pilot Hydrogen in Model Supersonic Combustors, *Journal of Propulsion and Power* Vol. 17, No. 6, 2001.
- S.P. Zeppieri, S.D. Klotz, F.L. Dryer, *Proc. Combust. Inst.* (28) (2000) 1587-1595

Figure 1. Effect of the CC inlet temperature on the flameholding (a) with related fuel composition (b).

Figure 2. Temperature distribution in the coupled system (a) with effect on the pyrolysis (b) and on the combustion (c) after 2.7 s of simulation (stabilised Mach 6 flight configuration with coolant flow rate of 10 g.s-1) and transient variation of methane production in the cooling channel (d).

Figure 3. Flame anchoring in the CC (a, c) and related OH formation (b, d) at different simulation times noted close to the curves for 1g .s-1 (a and b) and 10 g.s-1 (c and d).

Figure 4. Coolant mass flow effect on ignition in the CC (a) and on the fuel temperature (b).

Figure 5. Relationship between fuel flow rate and residence time in cooling channel (a) and hot face temperature (b).

Figure 6. Effect of coolant flow changes on fluids temperatures (a) with impact on the combustion process (b).

Figure 7. Effect of coolant flow changes on the fuel degradation (a) with consecutive hysteresis on acetylene formation (b).

Figure 8. Transient validation of numerical computations of CH<sub>4</sub> (a) and C<sub>3</sub>H<sub>8</sub> (b) formation computed with Dahm et al.'s (2004) and Dagaut and Cathonnet's (2006) mechanisms with FTIR measures during decane pyrolysis (60 bar, 0.1 g.s-1).

Figure 9. Experimental validation of Dagaut and Cathonnet's mechanism (2006) for decane and kerosene pyrolysis with GC/MS data (a) and comparison with previous Dahm et al.'s mechanism (2004) on gasification rate (b).

Table 1. Time characteristic of the phenomena in case of coolant flow rate gradient.

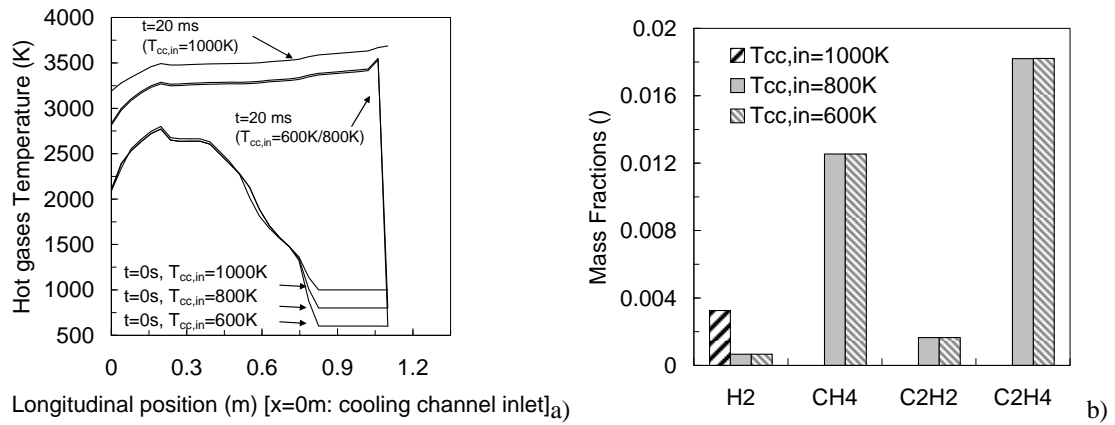
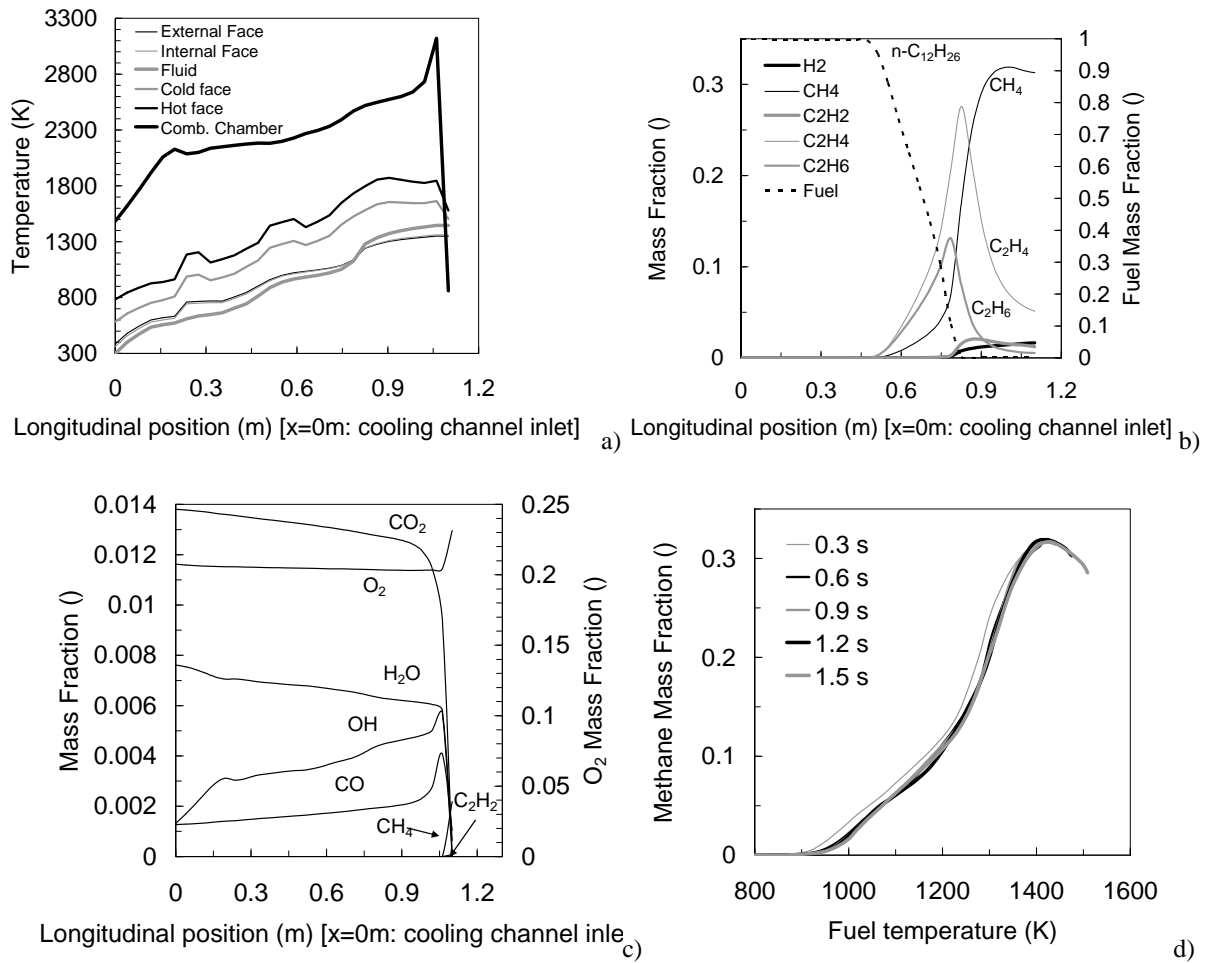
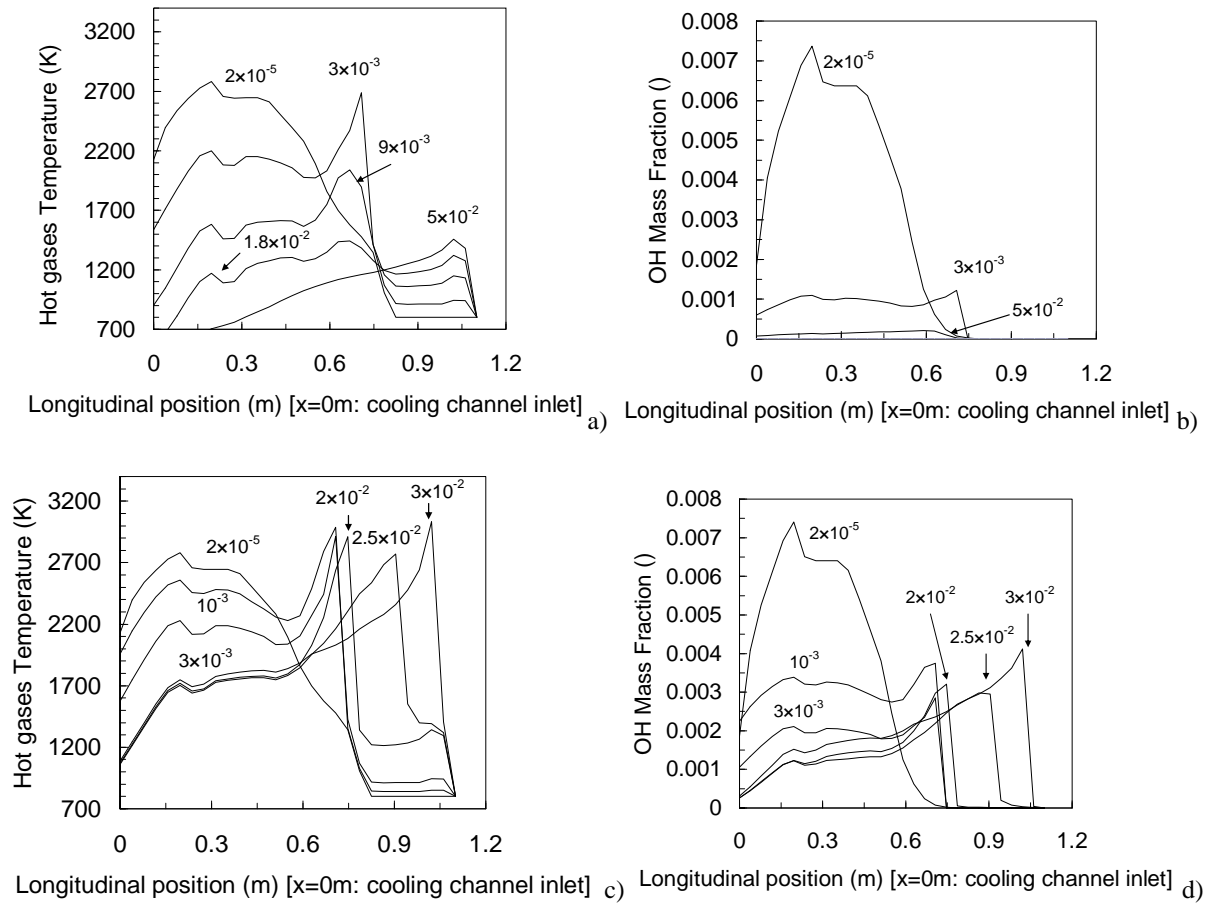


Figure 1. Effect of the CC inlet temperature on the flameholding (a) with related fuel composition (b).



**Figure 2. Temperature distribution in the coupled system (a) with effect on the pyrolysis (b) and on the combustion (c) after 2.7 s of simulation (stabilised Mach 6 flight configuration with coolant flow rate of 10 g.s<sup>-1</sup>) and transient variation of methane production in the cooling channel (d).**



**Figure 3. Flame anchoring in the CC (a, c) and related OH formation (b, d) at different simulation times noted close to the curves for  $1 \text{ g.s}^{-1}$  (a and b) and  $10 \text{ g.s}^{-1}$  (c and d).**

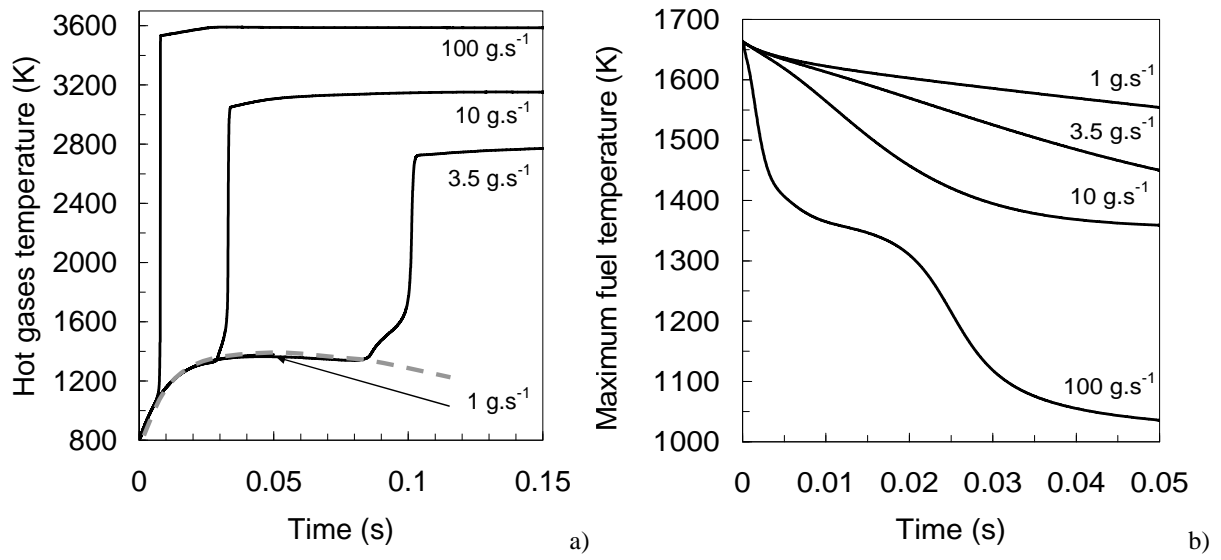


**Figure 4. Coolant mass flow effect on ignition in the CC (a) and on the fuel temperature (b).**

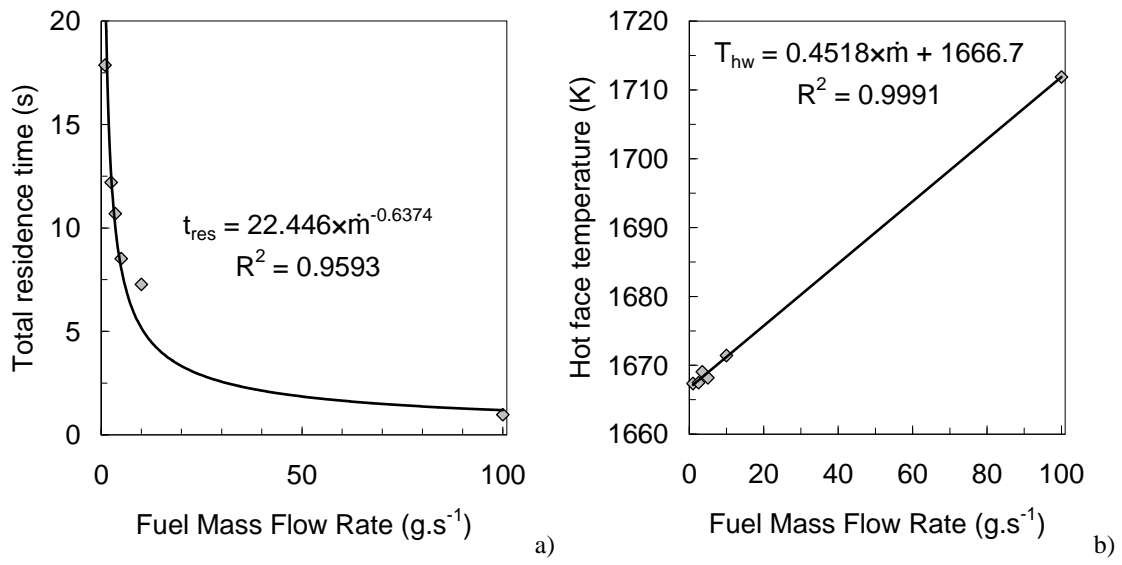


**Figure 5. Relationship between fuel flow rate and residence time in cooling channel (a) and hot face temperature (b).**

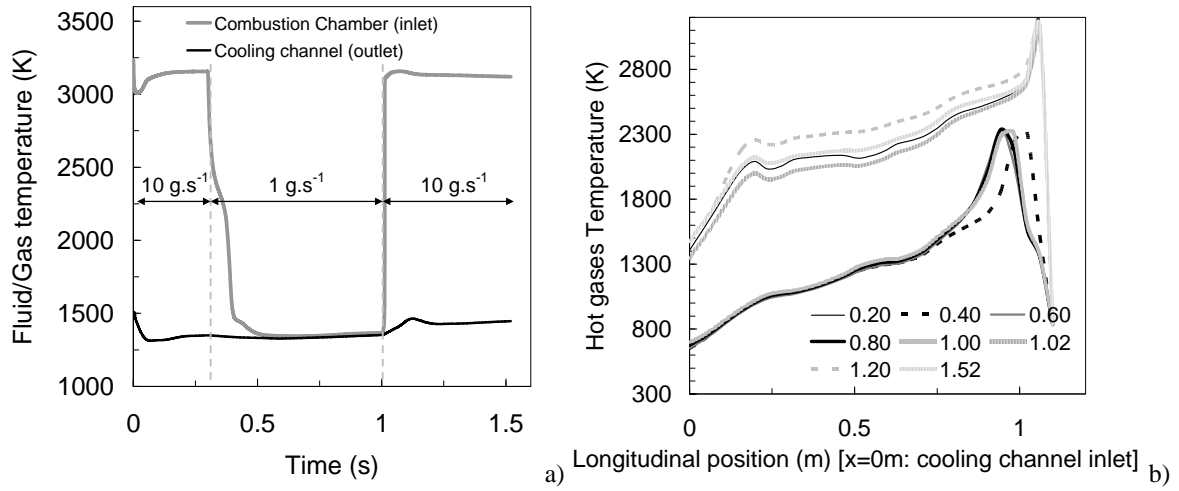


**Figure 6. Effect of coolant flow changes on fluids temperatures (a) with impact on the combustion process (b).**

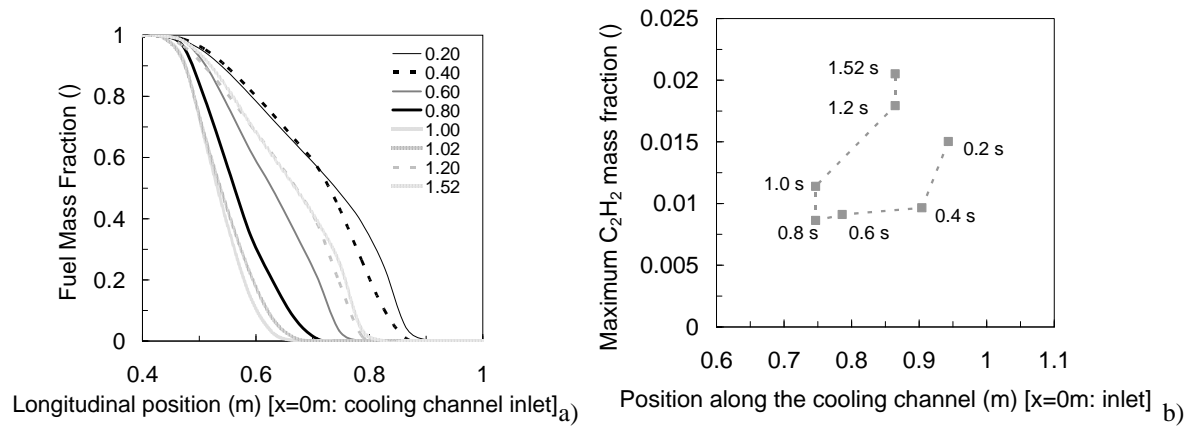


**Figure 7. Effect of coolant flow changes on the fuel degradation (a) with consecutive hysteresis on acetylene formation (b).**

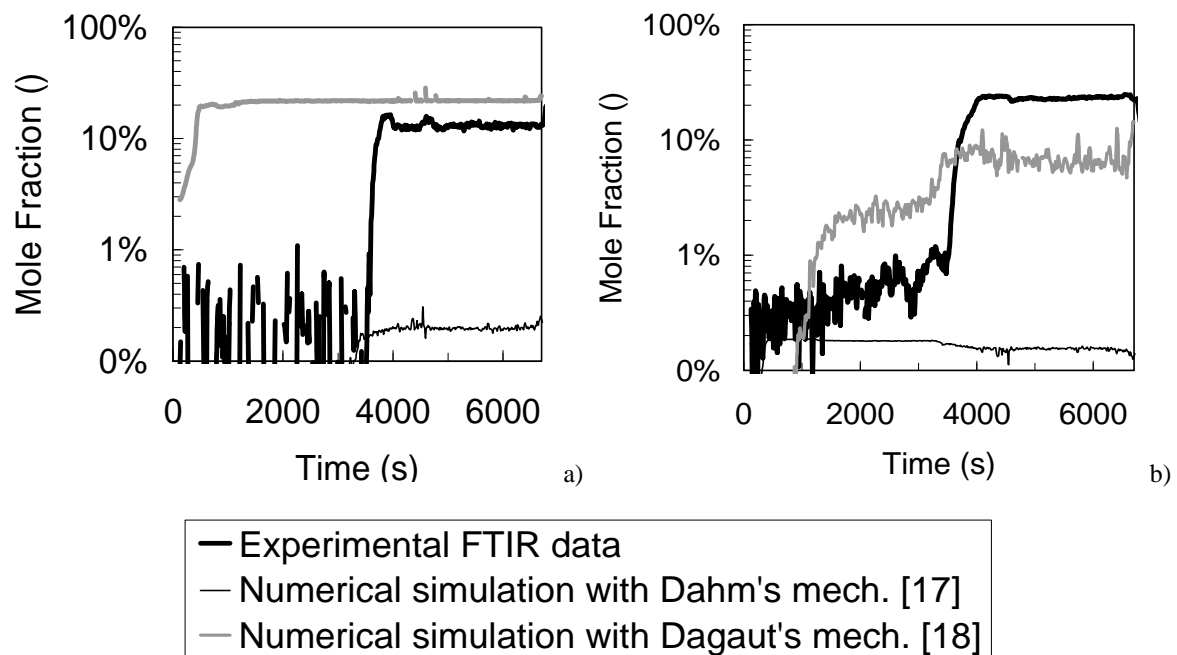


**Figure 8. Transient validation of numerical computations of  $\text{CH}_4$  (a) and  $\text{C}_3\text{H}_8$  (b) formation computed with Dahm et al.'s (2004) and Dagaut and Cathonnet's (2006) mechanisms with FTIR measures during decane pyrolysis (60 bar,  $0.1 \text{ g}\cdot\text{s}^{-1}$ ).**

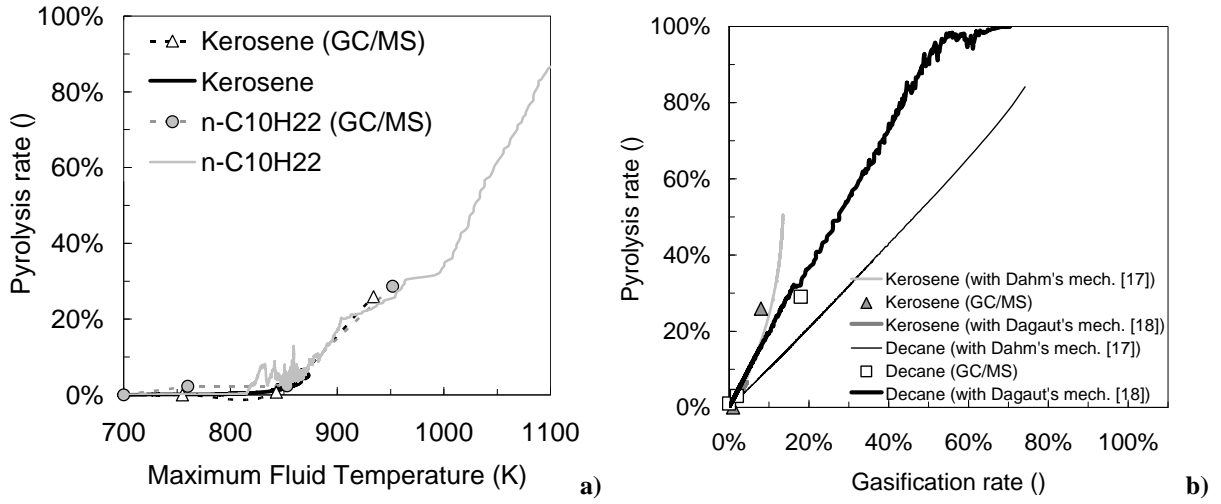


**Figure 9. Experimental validation of Dagaut and Cathonnet's mechanism (2006) for decane and kerosene pyrolysis with GC/MS data (a) and comparison with previous Dahm et al.'s mechanism (2004) on gasification rate (b).**

**Table 1. Time characteristic of the phenomena in case of coolant flow rate gradient.**

		0 s - 0.3 s	0.3 s - 1 s	1 s - 1.52 s
Temperature (K.s <sup>-1</sup> )	Combustion Chamber	-	7038	59000
	Cooling Channel	-	-	786
	Hot Wall	643	237	344
	Cold Wall	55	173	266
Mass Fraction (s <sup>-1</sup> )	Fuel conversion	1.27	0.32	1.56
	H2 formation	0.066	0.009	0.135
	OH formation	267	5.36	254
Mass flow rate (kg.s <sup>-2</sup> )	Cooling Channel	9		0.9